11

Coupled-Line Couplers Based on the Composite Right/Left-Handed (CRLH) Transmission Lines

Masoud Movahhedi and Rasool Keshavarz
Electrical Engineering Department, Shahid Bahonar University of Kerman, Kerman, Iran

1. Introduction

Recently, the idea of complex materials in which both the permittivity and the permeability possess negative real values at certain frequencies has received considerable attention. In 1967, Veselago theoretically investigated plane-wave propagation in a material whose permittivity and permeability were assumed to be simultaneously negative (Veselago, 1968). For materials with negative permittivity and permeability, several names and terminologies have been suggested, such as "left-handed" media, media with "negative refractive index" (NIR), "backward-wave" (BW) media and "double-negative"(DNG) material (Caloz & Itoh, 2005). In this book chapter, materials with negative permittivity and permeability, and hence negative index of refraction, will be referred indistinctly as left-handed metamaterials (LHMs) or metamaterials (MTMs) (Caloz & Itoh, 2005).

Metamaterials have found many applications in electromagnetic problems. For instance, numerous novel MTM-based microwave components have been proposed to control amplitudes, frequencies, and wave numbers of propagating and non-propagating electromagnetic modes (Caloz & Itoh, 2005). Advances in MTMs have also stimulated the development of new couplers with unique coupling mechanisms. Recently, coupled-line couplers (CLCs) using composite right/left-handed transmission lines (CRLH TLs), which are the special realization of transmission lines based on the metamaterial concept, with broad bandwidth and arbitrary loose/tight coupling levels have been developed. But usually these couplers occupy large length and also, because of using stubs in their structures, width of them would be large. For eliminating this drawback, we have proposed some new backward and forward coupled line couplers with high coupling levels, broad bandwidths and compact sizes, base on the CRLH TLs.

Organization of this chapter is as follows. In Section 2 theory of CRLH TLs, interdigital capacitor and their equivalent circuit models and parameters, have been explained. Section 3, at first, reviews some conventional CRLH- based CLCs and in continues presents our proposed couplers. In this section, three CLCs based on the concepts of CRLH CLCs are presented; a symmetrical backward CLC (Section 3.3.1), an asymmetrical backward CLC (Section 3.3.2) and a symmetrical forward CLC (Section 3.3.3).

2. Composite Right/Left Handed Transmission Lines (CRLH TLs)

A conventional transmission line (right-handed TL) is represented by a series inductance (L_R) and a shunt capacitance (C_R), implying the use of a low pass topology (Pozar, 2004). By interchanging the position of the inductor and capacitor, the resulting structure is referred to as left-handed TL with a high pass configuration (Caloz & Itoh, 2005). In these purely left-handed transmission lines (PLH TLs), the phase and group velocities are opposite to each other (Pozar, 2004). PLH TLs cannot exist physically because, even if we intentionally provide only series capacitance and shunt inductance, parasitic series inductance (L_L) and shunt capacitance (C_L) effects, increasing with increasing frequency, will unavoidably occur due to currents flowing in the metallization and voltage gradients developing between the metal patterns of the trace and the ground plane (Caloz & Itoh, 2002). Thus, the composite right and left handed (CRLH) model represents the most general MTM structure possible. Equivalent circuit model of a CRLH TL for one cell is shown in Fig. 1(a) (Caloz & Itoh, 2004a). In this figure, L_R and L_L are right and left handed inductances, respectively, also C_R and C_L are right and left handed capacitances, respectively. Many lumped (using SMT chip components) or distributed implementations (microstrip, stripline, CPW, etc.) are possible for CRLH TLs. Interdigital/stub configuration is one of widely used of these implementations (Caloz & Itoh, 2005). A layout of this configuration for one cell is shown in Fig. 1(b). A CRLH TL is constructed of these unit cells connected in series as shown in Fig. 1(c). This structure consists of series interdigital capacitor of capacitanceC_L and parallel short-ended stub working as inductor of inductance L_L. Moreover, L_R and C_R are parasitic elements of interdigital capacitor.

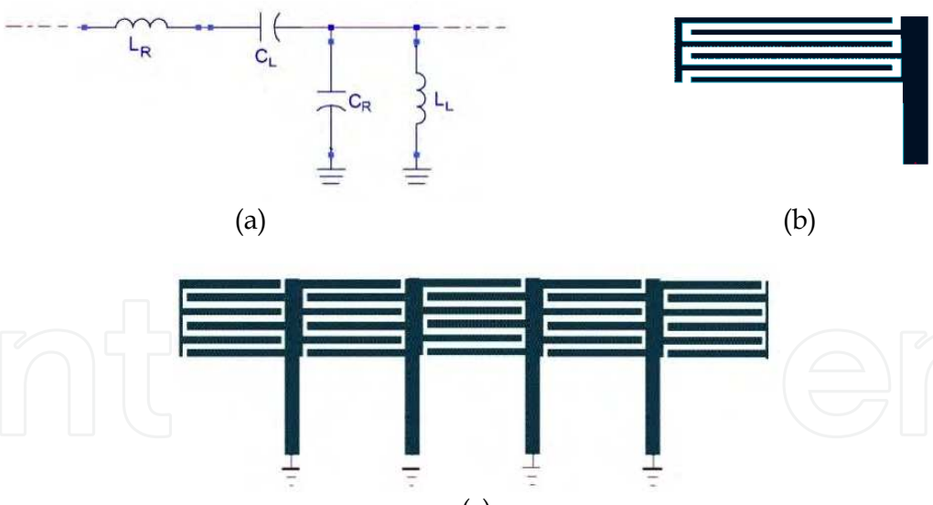

Fig. 1. (a) Equivalent circuit model of a CRLH TL for one cell. (b) Layout of a CRLH TL by using interdigital capacitor and shorted stub inductor for one cell. (c) Microstrip implementation of a CRLH TL.

An interdigital capacitor is a multifinger periodic structure which, as mentioned, can be used as a series capacitor in microstrip transmission lines technology (Bahl, 2003). This capacitor uses the capacitance that occurs across a narrow gap between thin-film conductors. Fig. 2 shows an interdigital capacitor and its equivalent circuit model. As seen

in this figure, an interdigital capacitor is made of some gaps. The gap meanders back and forth in a rectangular area forming two sets of fingers that are interdigital. These gaps are essentially very long and folded to use a small amount of area. By using a long gap in a small area, compact single-layer small-value series capacitors can be realized. Typically, its capacitance values range from 0.05 pF to about 0.5 pF. The capacitance can be increased by increasing the number of fingers, or by using a thin layer of high dielectric constant material such as a ferroelectric between the conductors and the substrate (Bahl, 2003).

The value of series capacitance of an interdigital structure can be expressed as (Bahl, 2003):

$$C_L = \frac{\varepsilon'_{re}}{18\pi}\,(N-1)\,\frac{K(\kappa)}{K'(\kappa)}\,l_s \qquad (pF) \tag{1}$$

where ε'_{re} is effective permittivity of a strip with width W, N is the number of fingers and $\frac{K(k)}{K'(k)}$ is a constant that has been presented in (Bahl, 2003).

As is well-known, the characteristic impedance of a CRLH TL (Z_c) with equivalent circuit model of Fig. 1(a) is given by (Caloz & Itoh, 2005):

$$Z_c = Z_L \sqrt{\frac{\left(\frac{\omega}{\omega_{se}}\right)^2 - 1}{\left(\frac{\omega}{\omega_{sh}}\right)^2 - 1}} \tag{2}$$

where

$$Z_L = \sqrt{\frac{L_L}{C_L}}\,,\ \omega_{se} = \frac{1}{\sqrt{L_R C_L}}\,,\ \omega_{sh} = \frac{1}{\sqrt{L_L C_R}} \tag{3}$$

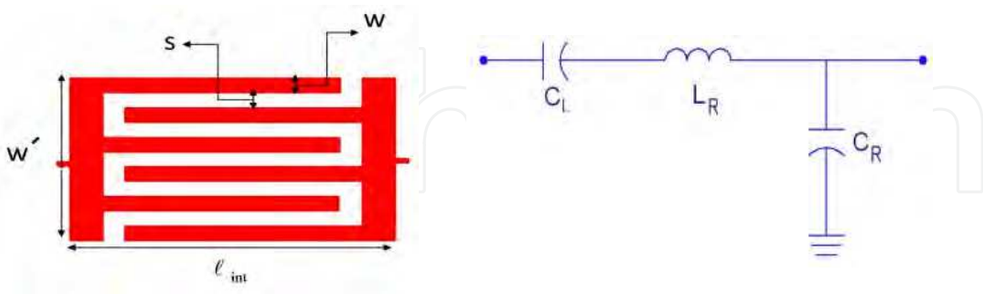

(a) (b)

Fig. 2. (a) Interdigital capacitor. (b) Its equivalent circuit model.

According to Fig. 2, the equivalent circuit model of an interdigital capacitor is similar to the equivalent circuit model of one cell of CRLH TL when $L_L \to \infty$. Inserting $L_L \to \infty$ into (2) results the characteristic impedance (Z_c^{int}) of a TL consists of cascaded interdigital capacitors as:

$$Z_c^{\text{int}} = \sqrt{\frac{\left(\frac{\omega}{\omega_{se}}\right)^2 - 1}{\omega^2 C_L C_R}} = \sqrt{\frac{L_R}{C_R} - \frac{1}{\omega^2 C_L C_R}} \tag{4}$$

It is seen from above equation that Z_c^{int} is real for $\omega > \omega_{se}$. From TL theory, it is clear that $\sqrt{L_R / C_R}$ is the characteristic impedance of a microstrip TL consists of a strip with width $W' = (4N-1)W$.

Similarly, the propagation constant for this TL is obtained as (Caloz & Itoh, 2005):

$$\beta^{\text{int}} = \sqrt{\omega^2 L_R C_R - \frac{C_R}{C_L}} \tag{5}$$

So, in a transmission line composed of interdigital capacitors which can be named ''interdigital transmission line'', for $\omega > \omega_{se}$, the propagation constant (β^{int}) is real and positive. It means that in this frequency interval, the interdigital transmission line operates in the right-handed (RH) band.

3. Coupled-Line Couplers (CLCs)

3.1 Conventional CLCs

Coupled line couplers are indispensable components in radio frequency (RF)/microwave communication systems. In these structures two unshielded transmission lines are close together, as indicated typically in Fig. 3, and power can be coupled between the lines. Such lines are referred to as coupled transmission lines (Mongia et al., 1999). The coupler is frequently utilized in a variety of circuits including modulators, balanced amplifiers, balanced mixers, and phase shifters. Rapidly expanding applications such as modern wireless technology continue to challenge couplers with extremely stringent requirements— high performance, broad bandwidth, and small size (Pozar, 2004).

In general, two types of CLCs have been proposed; backward and forward CLCs. When the coupled port is located on the same side of the structure as the input port and power is subsequently coupled backward to the direction of the source, this coupler is conventionally called a backward coupler and otherwise the CLC is called forward coupler (Mongia et al., 1999).

On the other hand, two types of edge-coupled backward CLCs have been presented. The first is the symmetrical coupler. When the two lines constituting a CLC are the same, the structure is called symmetric. In the symmetric structures, coupling mechanism is based on the difference between the characteristic impedances of the even and odd modes. The second one is the asymmetrical coupler. This coupler is asymmetrical as it is constituted of two different transmission lines. In this case, decomposition in even and odd modes is not possible anymore. The analysis becomes more difficult and the even/odd modes have to be replaced by the more general c and π modes, which are two fundamental independent modes, as described in (Mongia et al., 1999).

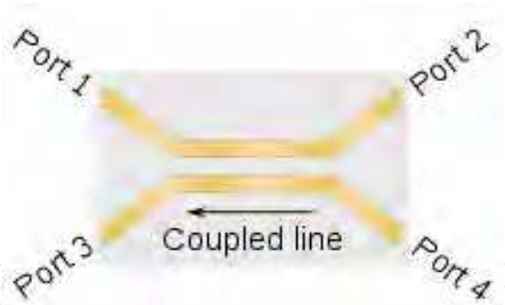

Fig. 3. Typical structure of a coupled-line coupler (CLC).

Symmetrical coupled lines represent a very useful but restricted class of couplers. In many practical cases, it might be more useful or even necessary to design components using asymmetrical coupled lines. For example, in some situations, the terminal impedance of one of the coupled lines may be different from those of the other. It may then be more useful to choose two coupled lines with different characteristic impedances. Also, an asymmetrical coupled-line coupler has usually broader bandwidth than symmetrical one (Mongia et al., 1999).

3.2 CRLH CLCs

The conventional CLC has several intrinsic drawbacks. First, their operating bandwidths are usually limited. Second, to raise the coupling level of a coupler, a very small space between the coupled lines is required and it is usually difficult to obtain due to fabrication constraints (Mongia et al., 1999).

As mentioned, in the past few years there has been a great interest in the field of metamaterials, especially composite right/left-handed structures (e.g. interdigital/stub configurations), and the microwave circuits based on the unusual properties of them (Caloz & Itoh, 2005). By closely placing two identical CRLH lines in parallel, such as configuration shown in Fig. 4, a strong contrast exists between the impedances of two fundamental modes of propagation (i.e. the even and odd mode impedances), which would result in high coupling-level.

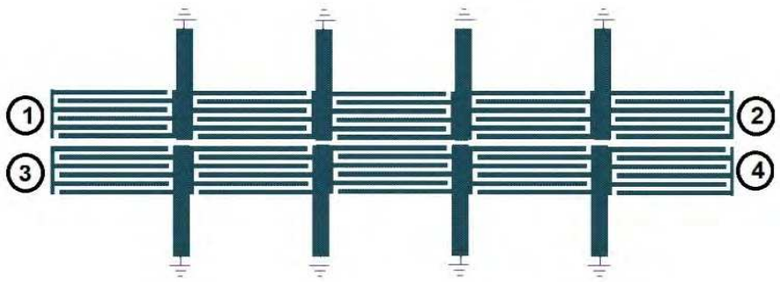

Fig. 4. Prototype of a CRLH edge-coupled directional coupler constituted of two interdigital/stub CRLH TLs.

For the first time, a novel composite right/left-handed coupled-line directional coupler composed of two CRLH TLs was proposed in (Caloz et al., 2004) and an even/odd-mode

theory was used to analyze the phenomenon of complete backward coupling. Then, an asymmetric RH-CRLH coupler was introduced and studied in (Caloz & Itoh, 2004b). It was composed of a conventional right-handed transmission line and a CRLH TL. That coupler showed the advantage of broad bandwidth and tight coupling characteristics, and coupled-mode theory based on traveling waves was used to discuss these interesting features. In (Islam & Eleftheriades, 2006), it was shown that the formation of a stop-band and the excitation of complex modes occurred in the case of coupling between a forward wave and a backward-wave mode for a range of frequencies around the tuning frequency. Moreover, authors in (Wang et al., 2007) presented the conditions for tight coupling and detailed formulas were given to define the edges of the coupling range.

Moreover, some CLCs based on the CRLH TLs with arbitrary coupling levels have been developed, recently (Fouda et al., 2010; Hirota et al., 2009; Hirota et al., 2011; Kawakami et al., 2010; Mocanu et al., 2010). In these couplers, the backward coupling depends on the difference between even and odd modes characteristic impedances and length of the coupled lines (Caloz & Itoh, 2005).

The interdigital/stub CLCs have been typically adapted to increasing coupling level, but these couplers increase in size (Caloz et al., 2004; Caloz & Itoh, 2004b; Islam & Eleftheriades, 2006), band width of them is narrow (Hirota et al., 2011; Mocanu et al. 2010; Wang et al. 2007) and the multiconductors of the interdigital construction complicate the design procedure (Caloz & Itoh, 2005).

It is considerable that the microstrip CRLH TL structures have been mostly implemented in the form of interdigital capacitors and stub inductors. In the other hand, using shorted stub inductors with large sizes to achieve the required inductances can cause the structure width to be also enlarged. For instance, the length and width of 3-dB microstrip coupled-line coupler proposed in (Caloz et al., 2004) are approximately $\lambda g/3$ and $\lambda g/6$, respectively. Also, bandwidth of the CRLH CLCs which presented in (Mocanu et al., 2010) and (Fouda et al., 2010) are 25% and 30%, respectively.

Also, forward coupling level in CRLH coupled line couplers is low (nearly -10 dB in (Fouda et al., 2010)).

3.3 Proposed CLCs

In this section, some of the authors' proposed CLCs based on the CRLH concepts to reach new couplers with better specifications, such as smaller size, broader bandwidth and more simplicity in fabrication are presented. In these new CLCs one has been trying to eliminate some drawbacks and disadvantages of conventional CRLH CLCs mentioned in previous section.

3.3.1 Backward symmetrical CLC

The proposed backward-wave directional coupler is shown in Fig. 5 (Keshavarz et al., 2011a). It is a coupled-line coupler consisting of an interdigital capacitor with one finger as a CRLH TL in each coupled-line. It is seen that using only one interdigital capacitor to realize the interdigital TLs is more suitable to reach a coupler with better matching and wider bandwidth. As it was mentioned, for $\omega > \omega_{se}$, these interdigital TLs will be operating

completely in their RH range for the presented coupler application. So in this coupler, similar to the conventional edge-coupled couplers, the coupling coefficient is (Pozar, 2004):

$$S_{31} = \frac{jk\sin\theta}{\sqrt{1-k^2}\cos\theta + j\sin\theta}, \quad k = \frac{Z_{ce} - Z_{co}}{Z_{ce} + Z_{co}} \tag{6}$$

where, $\theta=(2\pi l/\lambda g)$ is electrical length and ℓ is the length of CLC. Therefore, setting the interdigital capacitor length as $l= \lambda g/4$ or $\theta=\pi/2$ results in maximum coupling level. On the other hand, selection of $l= \lambda g/4$ preserves the homogeneity condition in CRLH structure (i.e., $p \le \frac{\lambda_g}{4}$, where p is structural cell size) (Caloz & Itoh, 2005).

The equivalent circuits model of the even and odd modes of Fig. 5 for one cell have been presented in Fig. 6. In this figure, L is the inductance for a strip with width W' and C_e, C_o are the distributed capacitances for the even and odd modes, respectively.

Even and odd mode characteristic impedances (Z_{ce}, Z_{co}) of the coupled-lines composed of interdigital TLs are obtained from (Caloz & Itoh, 2005) with setting $L_L \to \infty$ as:

$$Z_{ce} = \sqrt{\frac{L}{C_e} - \frac{1}{\omega^2 C_e C_L}} \quad , \quad Z_{co} = \sqrt{\frac{L}{C_o} - \frac{1}{\omega^2 C_o C_L}} \tag{7}$$

and

$$Z'_{ce} = \sqrt{\frac{L}{C_e}} \quad , \quad Z'_{co} = \sqrt{\frac{L}{C_o}} \tag{8}$$

Z'_{ce} and Z'_{co} are even and odd mode characteristic impedances of a conventional microstrip CLC with strips of width W' for each TL, where $W'(=(4N-1)W)$ is total width of the interdigital capacitor.

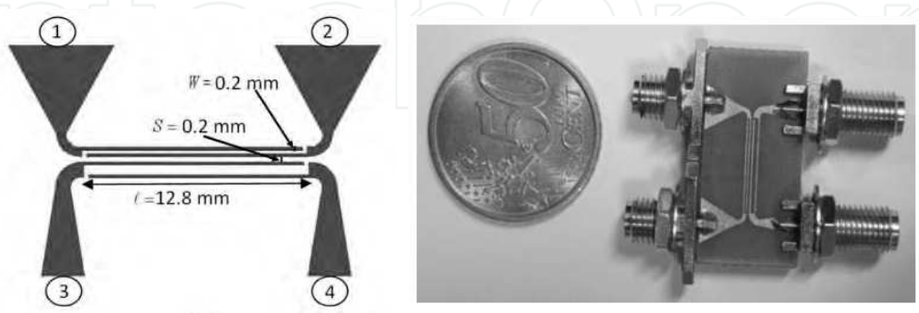

(a) (b)

Fig. 5. Structure of the proposed microstrip coupled-line backward coupler on FR4 substrate, $\varepsilon_r = 4.7$, thickness of 1.6 mm. (a) Structure layout. (b) Fabricated coupler (Keshavarz et al., 2011a).

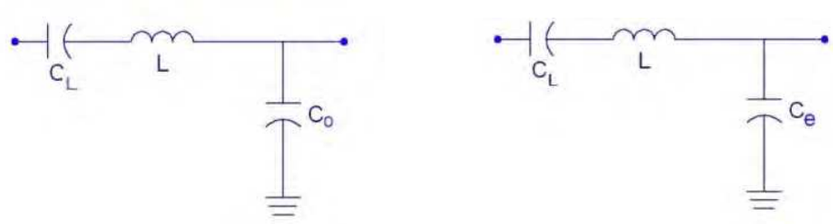

(a) (b)

Fig. 6. (a) Odd and (b) even modes equivalent circuit models of proposed coupler in Fig. 5 (Keshavarz et al., 2011a).

In the proposed coupler for given even and odd mode characteristic impedances, according to (7), selection of a small C_L leads to larger values of Z_{ce} and Z_{co}. This situation is very suitable for elimination of the fabrication restrictions in CLCs with tight coupling level. Consequently, to decrease the value of C_L in the proposed structure, interdigital capacitors with only one finger (i.e., N = 1) are used.

In design procedure, for an indicated coupling-level (c) and characteristic impedance (Z_c^{int}), Z_{ce} and Z_{co} can be obtained from conventional expressions as (Pozar, 2004):

$$Z_{ce} = Z_c^{\text{int}} \sqrt{\frac{1+c}{1-c}}, \quad Z_{co} = Z_c^{\text{int}} \sqrt{\frac{1-c}{1+c}} \tag{9}$$

With setting N = 1, $\ell = \lambda_g/4$ and the substrate profile being determined, C_L and C_R can be calculated using expressions presented in (Bahl, 2003) and Z'_{ce} and Z'_{co} are obtained from (7) and (8). Then, W' and S can be determined by using achieved Z'_{ce}, Z'_{co} and relative design graphs for conventional coupled microstrip lines.

For instant, Fig. 7(a) illustrates the required width of the interdigital TL (W) in the proposed coupler realized on FR4 substrate, with $\varepsilon_r = 4.7$ and thickness of 1.6 mm, for different values of Z'_{ce}. In addition, the necessary spacing between two coupled interdigital TLs (S) for the presented structure versus Z_m, where $Z_m = \dfrac{2Z'_{ce}Z'_{co}}{Z'_{ce} - Z'_{co}}$, has been provided in Fig. 7(b).

As it was mentioned, since Z'_{ce} and Z'_{co} would be larger than Z_{ce} and Z_{ce}, for constant coupling-level (c) and characteristic impedance (Z_c^{int}) in comparison with the conventional CLCs, W' decreases and S increases. Therefore in the proposed coupler, the fabrication constrains in conventional edge-coupled couplers to get a tight coupling-level caused very small spacing between two coupled lines (i.e., S) can be removed.

To validate the proposed technique, a 3-dB coupled line coupler based on the design procedure and presented expressions has been designed on FR4 substrate with $\varepsilon_r = 4.7$, thickness of 1.6 mm and *tan δ = 0.021*. Fig. 5 shows the designed coupler layout and the fabricated structure. A 3-dB coupled line coupler with nearly 60% bandwidth (from 2.3 to 4 GHz) around the design frequency f_c = 3.2 *GHz* is achieved in the measured prototype. The spacing between two TLs (S) and width of the interdigital capacitor fingers (W) are 0.2

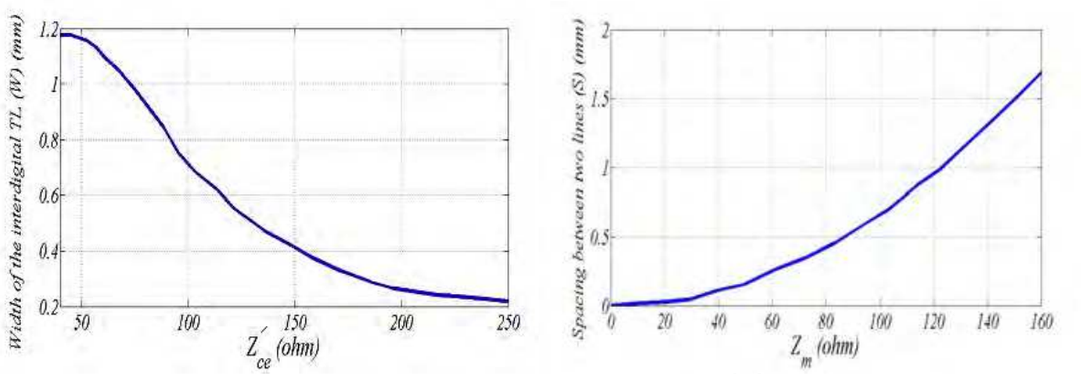

(a) (b)

Fig. 7. a) Width of the interdigital TL (*W*) versus Z'_{ce}, b) Spacing between two coupled interdigital TLs (*S*), in the proposed coupler on FR4 substrate, $\varepsilon_r = 4.7$, thickness of 1.6 mm (Keshavarz et al., 2011a).

mm. Also, the length of the TLs is 12.8 mm (see Fig.5). For better matching and wider bandwidth, we use only one interdigital capacitor, i.e. one cell, in every interdigital TL. Moreover, to reach a large isolation parameter, spacing between the fingers in the lower interdigital capacitor is set larger than the upper one, when ports 1 and 4 are the input and isolated ports, respectively. As shown in the layout of the coupler in Fig. 5, at the all four ports of the structure, tapered microstrip TLs have been used for the impedance matching to 50 Ω, as well as to fit the ports size to the inner conductors of the coaxial-to-microstrip transitions.

Fig. 8 presents the full-wave simulated (by using Agilent ADS software) and measured *S*-parameters for the coupler of Fig. 5. Excellent agreement can be observed between simulated and experimental results. There is only a small difference between S_{11} parameter of simulated and measurement results. Due to small distance between coupler connectors, we could not connect network analyzer ports to adjacent coupler connectors, directly. Therefore, two interface cables were connected to the coupler connectors and then *S*-parameters were measured. This drawback shows its bad effect on S_{11} parameter more strongly than other *S*-parameters.

Using these figures, a amplitude balance of ±2 dB over a bandwidth of 60% (2.3–4 GHz), a matching (10 dB bandwidth) and an isolation at least −20 dB over a bandwidth of 80% (2.2–4.6 GHz) are observed. Fig. 9 illustrates the phase difference between ports 2 and 3 of the coupler. This phase difference is 90^0 at design frequency and exhibits a phase-balance ($\pm 10^0$) bandwidth of 1.3 GHz.

In comparison with the conventional CRLH CLCs, the electrical length of the proposed CLC is more compact than the CRLH CLCs presented in (Islam et al., 2004; Mao & Wu, 2007; Nguyen & Caloz, 2006; Zhang et al., 2008). Moreover, due to the elimination of the stubs in the structure, its width is also smaller. For instance, the width of the coupler is nearly 11 times smaller than CRLH CLC reported in (Caloz et al., 2004) and its coupled-line electrical length is shortened to 60% of the 3-dB CRLH coupler electrical length presented in

(Keshavarz et al., 2011a). Moreover, the bandwidth of the proposed CLC is wider than CRLH CLCs presented in (Islam et al., 2004) and (Nguyen & Caloz, 2006).

In comparison with the conventional planar microstrip CLC realized in the same substrate material and similar spacing between coupled TLs, this CLC achieves higher coupling level. The high coupling level (8 dB or higher) is extremely difficult to achieve in the conventional CLC due to the present limit in fabrication (Pozar, 2004). Also, simulation results show that in the proposed structure if the spacing between the coupled lines increases, the bandwidth increases up to 85% for 7-dB coupling factor. Moreover, this coupler exhibits much higher design simplicity than the existing CRLH CLCs. Due to the wide bandwidth and compact size, the proposed coupler is well suitable for microwave and millimeter-wave integrated circuits, wideband communication systems and many kinds of antenna arrays.

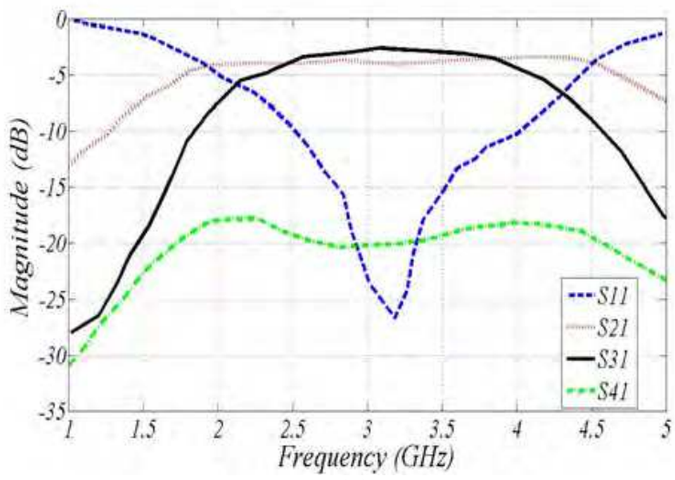

(a)

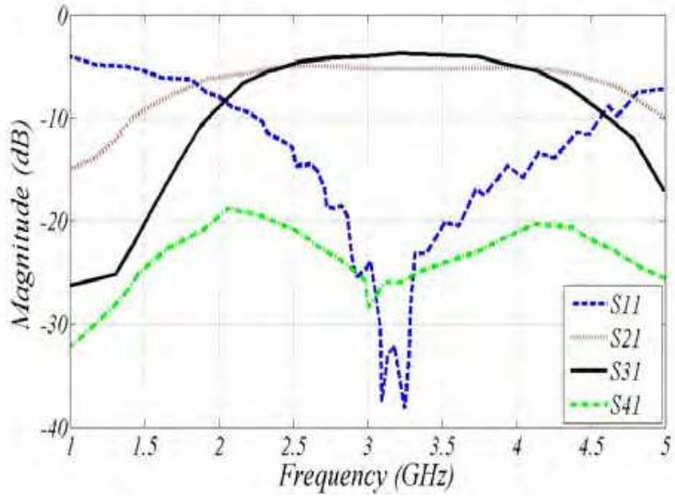

(b)

Fig. 8. *S*-parameters of the proposed coupler have shown in Fig.5 (a) Full-wave simulation results. (b) Measurement results (Keshavarz et al., 2011a).

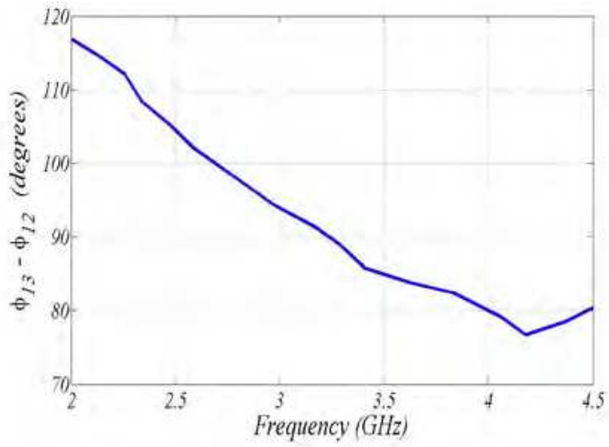

Fig. 9. Measured phase difference between the through port and the coupled port for the proposed coupler of Fig. 5 (Keshavarz et al., 2011a).

3.3.2 Backward asymmetrical CLC

In this section, an asymmetrical coupled-line coupler based on the interdigital TL is presented. Fig. 10 shows layout and circuit model of the interdigital TL and conventional TL which are adjacent to each other as asymmetrical backward coupled-line coupler. As depicted in Fig. 10(b), C_m represents the mutual capacitance between interdigital and strip of the microstrip conductors in the absence of the structure ground conductor while C_1 and C_2 represent the capacitance between interdigital or microstrip strip conductors and ground, respectively. Moreover, the circuit model includes mutual inductance (L_m) and self-inductances of interdigital (line 1) and conventional microstrip (line 2) conductors, i.e. L_1 and L_2, respectively. C_{int} is series interdigital capacitor of line 1. It should be stated that all of parameters in the circuit model are per unit length quantities. Also, Fig. 11 shows the capacitance representation for quasi-TEM mode of cross section of the proposed asymmetrical coupler. For structure analysis, it is assumed that lines 1 and 2 are terminated to impedances Z_a and Z_b, respectively.

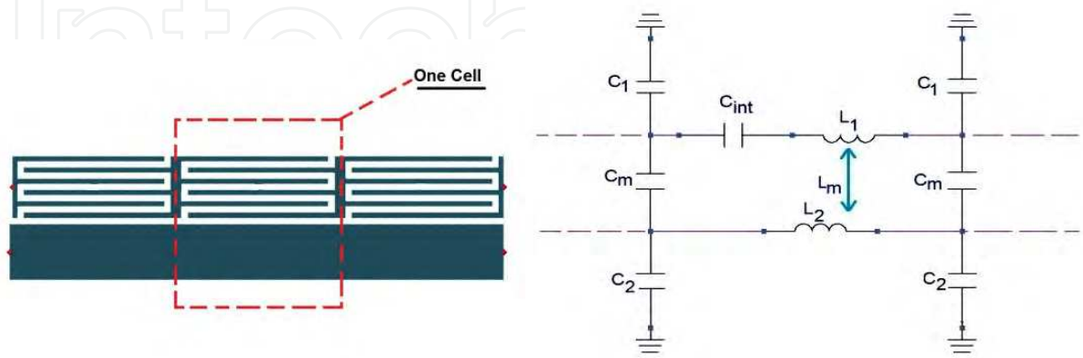

(a) (b)

Fig. 10. Proposed asymmetrical coupled-line coupler consisted of interdigital TL and microstrip conventional TL. a) Its layout and b) lumped equivalent circuit model.

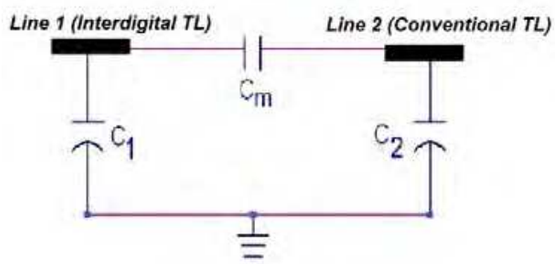

Fig. 11. Capacitance representation for cross section of the asymmetrical coupler presented in Fig. 10.

Characteristics of the proposed coupled transmission line can be described by a superposition of characteristics of c and π modes. A set of two coupled lines can support two fundamental independent modes of propagation (called normal modes). For asymmetrical coupled lines, the two normal modes of propagation are known as c and π modes (Mongia et al., 1999). Both c and π modes are composed of two traveling waves in the backward and forward directions. The c mode is characterized by four parameters: γ_c, Z_{c1}, Z_{c2} and R_c which are the propagation constant of the mode, the characteristic impedances of lines 1 and 2 and the ratio of the voltages on the two lines of the c mode, respectively. Similarly, the π mode is also characterized by four parameters: γ_π, $Z_{\pi 1}$, $Z_{\pi 2}$ and R_π which are propagation constant of the mode, characteristic impedances of lines 1 and 2 and the ratio of the voltages on the two lines of the π mode, respectively (Mongia et al., 1999).

As it has been shown in (Mongia et al., 1999), the relation between the characteristic impedances, i.e. Z_{c1}, Z_{c2}, $Z_{\pi 1}$ and $Z_{\pi 2}$, and also the ratio parameters, i.e. R_c and R_π, are as:

$$\frac{Z_{c2}}{Z_{c1}} = \frac{Z_{\pi 2}}{Z_{\pi 1}} = -R_c R_\pi \tag{10}$$

So, a total number of only six quantities, i.e. γ_c, γ_π, Z_{c1} or Z_{c2}, $Z_{\pi 1}$ or $Z_{\pi 2}$, R_c and R_π are required to characterize asymmetrical coupled lines. For a lossless TEM-mode coupled-line, the propagation constants of both c and π modes are the same, and are given by (Cristal, 1966):

$$\gamma_c = \gamma_\pi = j\beta \tag{11}$$

As special case for asymmetrical coupled lines, symmetrical coupled line are completely characterized by four parameters, the even and odd modes characteristic impedances of any lines (as both lines are identical) and even and odd modes propagation constants. In symmetrical coupled lines, R_c and R_π are equal to 1 and -1, respectively (Mongia et al., 1999).

By assuming the quasi-TEM mode for proposed structure and according to equations (10), (11) and (Cristal, 1966) for above asymmetrical coupler (Fig. 10), it is obtained that:

$$R_c = -R_\pi = \sqrt{\frac{Z_2}{Z_1}} \tag{12}$$

where

$$Z_1 = \sqrt{\frac{L_1}{C_1} - \frac{1}{\omega^2 C_{\text{int}} C_1}} \quad , \quad Z_2 = \sqrt{\frac{L_2}{C_2}} \tag{13}$$

where Z_1 and Z_2 are characteristic impedances of uncoupled lines 1 (interdigital TL) and 2 (conventional microstrip TL), respectively.

Moreover, the capacitance matrix of the coupled lines (Fig. 10) can be expressed as (Cristal, 1966):

$$[C] = \begin{bmatrix} C_1 & C_{12} \\ C_{21} & C_2 \end{bmatrix} = \begin{bmatrix} C_1 + C_m & -C_m \\ -C_m & C_2 + C_m \end{bmatrix} \tag{14}$$

According to equations (13) and (14), c and π mode characteristic impedances of interdigital transmission line (${Z_{0c}}^a, {Z_{0\pi}}^a$) and the conventional microstrip transmission line (${Z_{0c}}^b, {Z_{0\pi}}^b$) are obtained as (Cristal, 1966):

$$\begin{cases} {Z_{0c}}^a = \sqrt{\dfrac{L_1}{C_1} - \dfrac{1}{\omega^2 C_{\text{int}} C_1}} \\ {Z_{0\pi}}^a = \sqrt{\dfrac{L_1}{(C_1 + 2C_m)} - \dfrac{1}{\omega^2 C_{\text{int}} (C_1 + 2C_m)}} \\ {Z_{0c}}^b = \sqrt{\dfrac{L_2}{C_2}} \\ {Z_{0\pi}}^b = \sqrt{\dfrac{L_2}{C_2 + 2C_m}} \end{cases} \tag{15}$$

and

$${Z'_{0c}}^a = \sqrt{\frac{L_1}{C_1}} \quad , \quad {Z'_{0\pi}}^a = \sqrt{\frac{L_1}{(C_1 + 2C_m)}} \tag{16}$$

${Z'_{0c}}^a$ and ${Z'_{0\pi}}^a$ are c and π mode characteristic impedances of a conventional microstrip TL with a strip of width W', where W' (= $(2N-1)S' + 2NW$) is the total width of the interdigital capacitor.

In coupler design procedure, for an indicated coupling-level (k) and impedance ports Z_a and Z_b of lines 1 and 2, respectively, ${Z_{0c}}^a, {Z_{0\pi}}^a, {Z_{0c}}^b$ and ${Z_{0\pi}}^b$ can be calculated from following equations (Cristal, 1966):

$$\begin{cases} {Z_{0c}}^{a} = \dfrac{Z_a Z_b \sqrt{1-k^2}}{Z_b - k\sqrt{Z_a Z_b}} \\ {Z_{0\pi}}^{a} = \dfrac{Z_a Z_b \sqrt{1-k^2}}{Z_b + k\sqrt{Z_a Z_b}} \\ {Z_{0c}}^{b} = \dfrac{Z_a Z_b \sqrt{1-k^2}}{Z_a - k\sqrt{Z_a Z_b}} \\ {Z_{0\pi}}^{b} = \dfrac{Z_a Z_b \sqrt{1-k^2}}{Z_a + k\sqrt{Z_a Z_b}} \end{cases} \tag{17}$$

In order the values of ${Z_{0c}}^{a}$ and ${Z_{0c}}^{b}$ to be positive, it is necessary that:

$$\frac{1}{k^2} \geq \frac{Z_a}{Z_b} \quad \text{and} \quad \frac{1}{k^2} \geq \frac{Z_b}{Z_a} \tag{18}$$

where k^2 denotes the power coupling coefficient between two coupled lines.

As it was mentioned, for indicated coupling level (k) and ports impedance (Z_a, Z_b) in the proposed coupler, the c and π characteristic impedances, i.e. ${Z_{0c}}^{a}, {Z_{0\pi}}^{a}, {Z_{0c}}^{b}$ and ${Z_{0\pi}}^{b}$, can be determined using (17). It is clear from (15) that selecting a small C_{int} in the introduced coupler, increases values of ${Z'_{0c}}^{a}$ and ${Z'_{0\pi}}^{a}$ which can lead to smaller value for C_m. It means that in this situation, the required spacing between two coupled-lines can be increased in comparison with the conventional microstrip coupled-lines. It is due to the inverse relationship between mutual capacitance value and spacing between coupled lines. Therefore, it is suitable for realizing high coupling-level coupled-line couplers with relatively larger spacing between two lines than conventional coupled-line couplers.

Fig. 12 illustrates the layout and fabrication of the proposed asymmetrical coupler that above considerations have been considered in its design (Keshavarz et al., 2011b).

For an asymmetric coupled microstrip line of the type shown in Fig. 12, the design graphs presented in Figs. 13, 14 and 15 can be used to determine the necessary interdigital and microstrip strip widths and spacing for a given set of characteristic impedances, ${Z_{oc}}^{a}, {Z_{0c}}^{b}$ and Z_m on FR-4 substrate with $\varepsilon_r = 4.6$ and thickness of 1.6 mm. In Fig. 15, Z_m is defined as:

$$Z_m = \frac{2{Z_{0c}}^{b}{Z_{0\pi}}^{b}}{{Z_{0c}}^{b} - {Z_{0\pi}}^{b}} \tag{19}$$

The asymmetrical coupled line coupler presented in this study is a 3-dB coupler at center frequency of 3 GHz which is simulated on FR-4 substrate with 1.6 mm substrate thickness and a dielectric constant of 4.6. Impedances of all four ports have been considered equal to $50\,\Omega$ $(Z_a = Z_b = 50\,\Omega)$. The final structure of designed coupler has been presented in Fig. 12(b) with $W_1 = 0.6\ mm, W_2 = 1\ mm$ and the spacing between two coupled lines (s) is 0.2 mm.

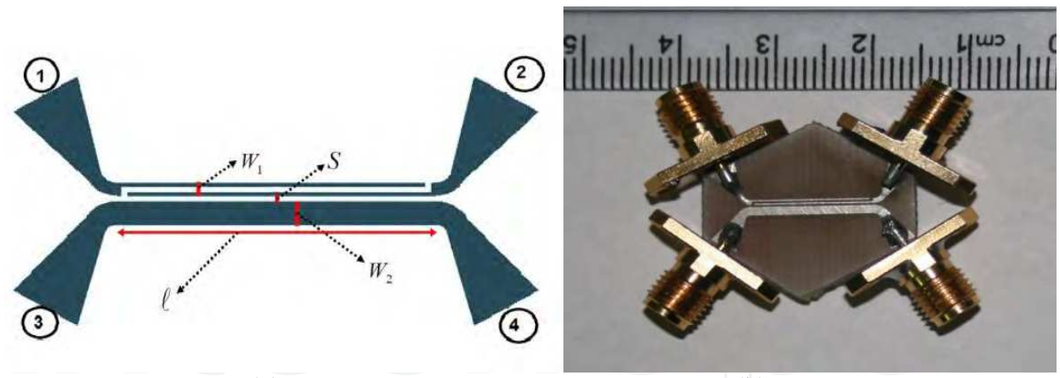

(a) (b)

Fig. 12. Proposed asymmetrical backward coupler based on the interdigital and conventional microstrip coupled TLs. (a) Structure layout. (b) Fabricated coupler. (Keshavarz et al., 2011b).

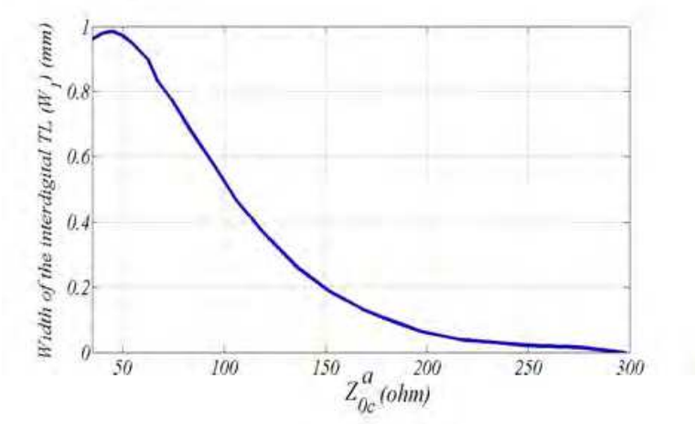

Fig. 13. Design graph for width of the interdigital TL (W_1) on FR-4 substrate versus *c* mode characteristic impedance. (Keshavarz et al., 2011b).

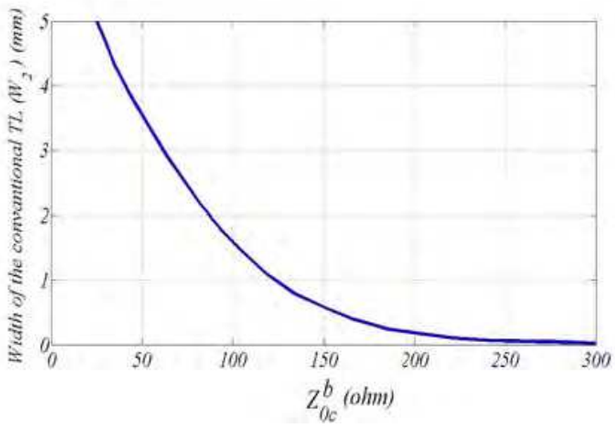

Fig. 14. Design graph for width of the conventional microstrip TL (W_2) on FR-4 substrate versus *c* mode characteristic impedance. (Keshavarz et al., 2011b).

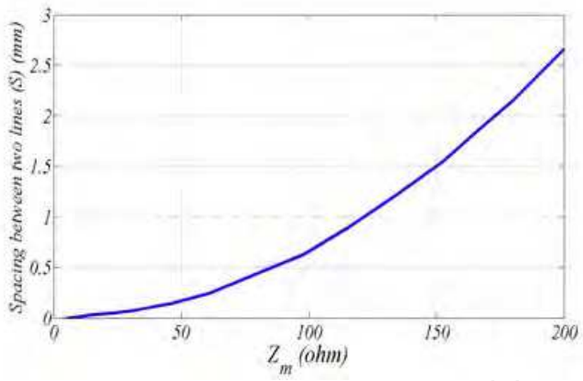

Fig. 15. Design graph for two lines separation (S) on FR-4 substrate versus Z_m . (Keshavarz et al., 2011b).

So, this coupler is more compact than CRLH coupled line couplers reported in (Abdelaziz et al., 2009; Garcia-Perez et al., 2010; Joon-Boom et al., 2001), due to the elimination of the stubs. The structure coupled-line length (ℓ) is equal to 12 mm, which is approximately $\lambda_g/4$ at center frequency of 3 GHz and is smaller than the CRLH microstrip CLC with the coupled line length around $\lambda_g/3$ (Caloz et al., 2004).

In addition to the equivalent circuit model which is used to simulate the designed coupler, a full-wave electromagnetic simulator (ADS) is also used to examine the structure. Fig. 16 illustrates the full-wave and equivalent circuit model analysis results of the proposed asymmetric backward coupler along with its measured S-parameters. Excellent agreement can be observed between full-wave simulated and experimental results. The elements of the equivalent circuit model are obtained using equations (13) and (15) and for this example are equal to $L_1 = 7.33\,nH$, $C_1 = 0.7\,pF$, $C_{\text{int}} = 1.82\,pF$, $L_2 = 6.18\,nH$, $C_2 = 0.86\,pF$. Using this figure, performance of the introduced 3-dB edge-coupled coupled-line coupler can be stated as the following: the power which is coupled to port 3 is approximately -3 dB, the return loss is less than -14 dB and the isolation is better than -13 dB over the bandwidth of 66% from 2.2 GHz to 4.2 GHz. Moreover, Fig. 17 shows the phase difference between the ports 2 and 3 of the coupler. As it is seen, this difference is equal to $90 \pm 10°$ for a frequency range from 2.2 GHz to 3.5 GHz. Proposed asymmetrical backward coupler exhibits reachable dimension, broad bandwidth and smaller size than the conventional and CRLH couplers.

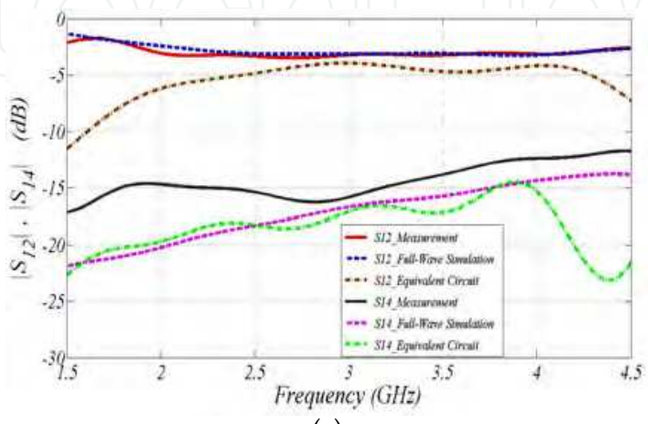

(a)

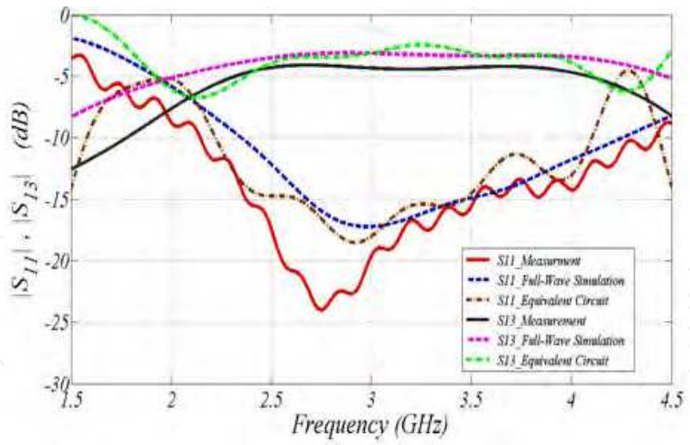

(b)

Fig. 16. Magnitude of the S-parameters for the proposed coupler obtained by full-wave simulation, equivalent circuit model and measurement results. (a) $|S_{12}|$,$|S_{14}|$ (b) $|S_{11}|$,$|S_{13}|$ (Keshavarz et al., 2011b).

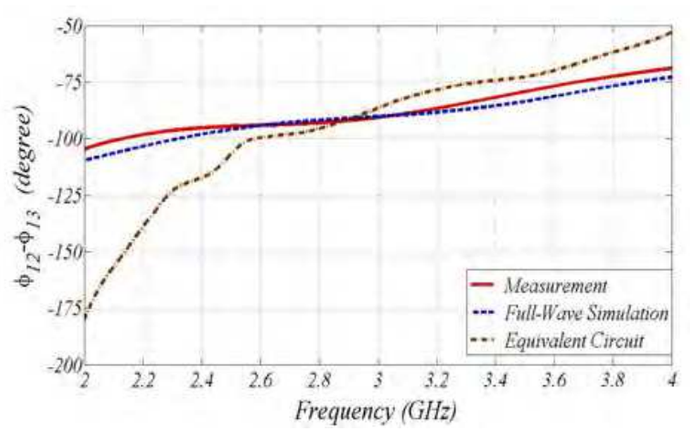

Fig. 17. Phase difference between the through and the coupled ports for the proposed coupler of Fig. 12. (Keshavarz et al., 2011b).

3.3.3 Forward symmetrical CLC

The scattering parameters of an ideal forward-wave directional coupler, as shown in Fig. 3, are given by (Mongia et al., 1999):

$$\begin{cases} S_{11} = 0 \\ S_{12} = -je^{\frac{-j(\beta_e+\beta_o)l}{2}} \cos[\frac{(\beta_e-\beta_o)l}{2}] \\ S_{13} = 0 \\ S_{14} = -je^{\frac{-j(\beta_e+\beta_o)l}{2}} \sin[\frac{(\beta_e-\beta_o)l}{2}] \end{cases} \quad (20)$$

where β_e and β_o are even and odd mode propagation constants of coupled lines, respectively. Also, l is length of the coupled line. As it was mentioned, forward-wave directional couplers cannot be realized using TEM mode transmission lines such as coaxial lines. It is due to this fact that for the TEM mode, the propagation constant of the even and odd modes are equal, and as shown in (20), there is no coupling between ports 1 and 4. Therefore, forward-wave coupling mechanism can only be appeared in non-TEM coupled TLs such as metallic waveguides, fin lines, dielectric waveguides and also quasi-TEM mode TLs like microstrip lines at high operating frequencies. In these transmission line structures, in general, the phase velocities of the even and odd modes are not equal (Mongia et al., 1999).

From (20), it is clear that complete power can be transferred between lines if the length l of the coupled line is chosen as:

$$l = \frac{\pi}{|\beta_e - \beta_o|} \tag{21}$$

Above result is significant in the sense that even for arbitrarily small values of difference in the propagation constants of even and odd modes, complete power can be transformed between the lines if the length of the coupler is chosen according to (21). In this situation, the directivity and isolation of the coupler are thus infinite. Also, the phase difference between ports 1 and 4 (S_{41} and S_{21}) is 90°. However, in general, situation (21) cannot be completely satisfied. Hence, some finite amount of backward-wave coupling always exists between coupled lines.

Our proposed forward-wave coupled-line coupler is shown in Fig. 18(a), where the coupled-lines have the same width of W and periodic stubs have been loaded between these coupled-lines (Keshavarz et al., 2010). In this structure, W_s and ℓ_s are the width and length of the periodic stubs, respectively, and d_s is a period of the stubs. The mid plane (red line in Fig. 18(a)) between the coupled-lines remains two different equivalent circuits for the even and odd modes. The even and odd modes are associated with a magnetic wall (open-circuit) and an electric wall (short-circuit), respectively. These two equivalent circuit models have been presented in Figs. 18(b) and 18(c) for one period. In these circuits, C_e and C_o are even and odd mode capacitances per unit length, respectively, and L is inductance per unit length of the coupled-lines. C_e and C_o are equal to:

$$C_e = C_{11} = C_{22}, \quad C_o = C_{11} + 2C_{12} + C_{\text{int}} \tag{22}$$

where C_{11} and C_{22} represent the capacitance between one strip conductor and ground in absence of the other strip conductor, in planar structures. Because of the strip conductors of the coupled lines are identical in size and location relative to the ground conductor, C_{11} will be equal to C_{22} or $C_{11} = C_{22}$. From transmission line theory, it is well known that the value of C_{11} is (Pozar, 2004):

$$C_{11} = \frac{\sqrt{\varepsilon_{re}}\, Z}{c} \tag{23}$$

where ε_{re} is effective permittivity of a microstrip transmission line with a strip with width W, Z is characteristic impedance of the transmission line and c is the speed of light. Also, C_{12} represents the capacitance between the two coupled lines without stubs and ground conductor. C_{int} is capacitance per unit length of the interdigital capacitor formed between the two coupled lines.

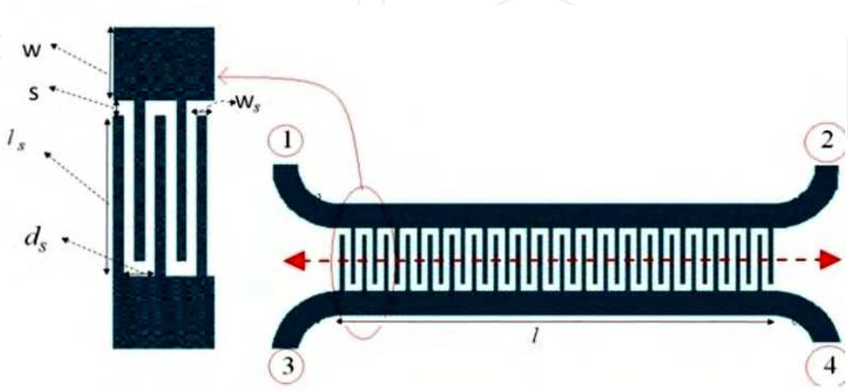

(a)

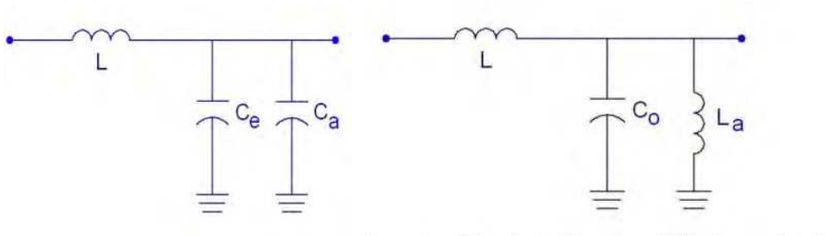

(b) (c)

Fig. 18. (a) Proposed forward-wave coupled-line coupler with periodic stubs. (b) Even mode, and (c) odd mode equivalent circuit models of each coupled line for one period (Keshavarz et al., 2010).

Some extra distributed shunt capacitance and inductance per unit length are added to the equivalent circuit models for the even and odd modes, respectively, which are given based on the TL theory as (Pozar, 2004):

$$L_a = \frac{1}{d_s}\left(\frac{Z_s}{\omega}\tan\beta_s\left(\frac{l_s+s}{2}\right)\right) \approx \frac{Z_s\beta_s(l_s+s)}{2\omega d_s}$$
$$C_a = \frac{1}{d_s}\left(\frac{1}{\omega Z_s}\tan\beta_s\left(\frac{l_s+s}{2}\right)\right) \approx \frac{\beta_s(l_s+s)}{2\omega Z_s d_s} \quad (24)$$

where Z_s and β_s represent characteristic impedance and phase constant of the shunt stubs, respectively.

Series impedance and shunt admittance of these equivalent circuit models in even and odd modes are given by:

$$\begin{aligned} Z_e &= j\omega L, \quad Y_e = j\omega(C_e + C_a) \\ Z_o &= j\omega L, \quad Y_o = j\omega C_o + 1/j\omega L_a \end{aligned} \tag{25}$$

According to the TL theory, the propagation constants and the characteristic impedances of the transmission coupled-lines in even and odd modes are:

$$\begin{aligned} \gamma_e &= \sqrt{Z_e Y_e} = j\omega\sqrt{L(C_e + C_a)} = j\beta_e \\ \gamma_o &= \sqrt{Z_o Y_o} = j\omega\sqrt{L(C_o - 1/\omega^2 L_a)} = j\beta_o \end{aligned} \tag{26}$$

and

$$\begin{aligned} Z_{ce} &= \sqrt{\frac{Z_e}{Y_e}} = \sqrt{\frac{j\omega L}{j\omega(C_e + C_a)}} = \sqrt{\frac{L}{(C_e + C_a)}} \\ Z_{co} &= \sqrt{\frac{Z_o}{Y_o}} = \sqrt{\frac{j\omega L}{j\omega(C_o - 1/\omega^2 L_a)}} = \sqrt{\frac{L}{(C_o - 1/\omega^2 L_a)}} \end{aligned} \tag{27}$$

Since, the length of the stubs is relatively large, the value of C_{12} would be very smaller than C_{11} and C_{int}. So, (22) can be approximated as:

$$C_o \cong C_{11} + 2C_{\text{int}} \tag{28}$$

As it is seen in (26), the difference between β_e and β_o in proposed structure becomes larger than conventional structures without stubs in coupled line couplers. Moreover, this difference can be controlled by stub length, so that for a fixed coupling-level, increasing length of stubs (ℓ_s) results reduction of structure length (Fig. 19).

In the coupled-line couplers, input matching condition for termination of impedance $Z_c (Z_{in} = Z_c)$ is achieved under condition which is given by (12).

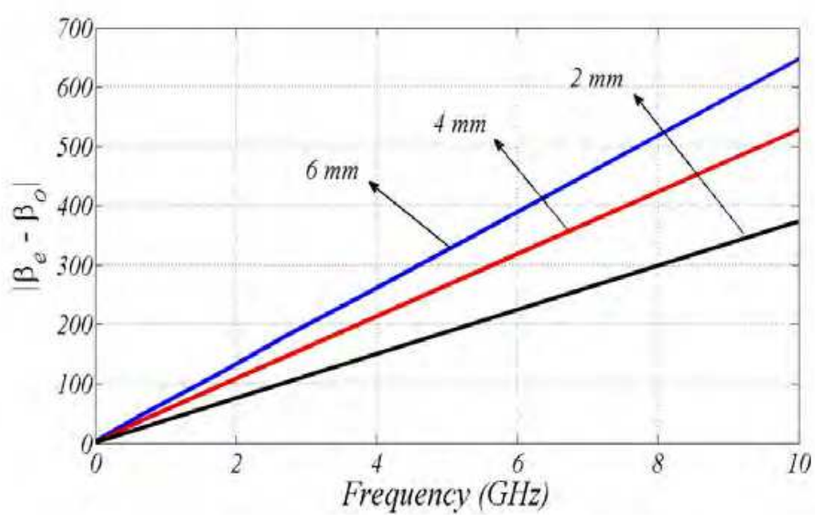

Fig. 19. $|\beta_e - \beta_o|$ for three lengths of the stubs ($l_s = 2, 4$ *and* 6 *mm*) (Keshavarz et al., 2010).

Fig. 20 presents some curves for selecting dimension of the proposed coupler for three coupling-levels (0-dB, 3-dB and 6-dB) with $W_s = 0.2\,mm$, $d_s = 0.6\,mm$ and $S = 0.2\,mm$ on FR-4 substrate ($\varepsilon_r = 4.6$, $h = 1.6\,mm$). These curves illustrate that with increasing the coupling-level, dimension of the coupler increase. But, it is interesting to note that for a fixed coupling-level, the area of the coupler (product of the stub length by the structure length) will remain constant, approximately.

The proposed structure of the forward-wave CLC in this section is fabricated on FR4 substrate with 1.6 mm thickness and dielectric constant of 4.6, as shown in Fig. 21. The full-wave simulator Agilent Technologies Advanced Design System (ADS) is used to examine the structure. For good matching, the width of the microstrip transmission lines for 50Ω port impedances is selected equal to 1 mm (i.e. $W = 1\,mm$). To have a coupling level of 0-dB, according to the derived relations and Fig. 20, the length (l) and width ($l_s + 2W$) of the structure in Fig. 18 have been chosen equal to 26 mm and 4 mm, which are approximately $\lambda_g/2$ and $\lambda_g/13$ at center frequency of 3 GH, respectively.

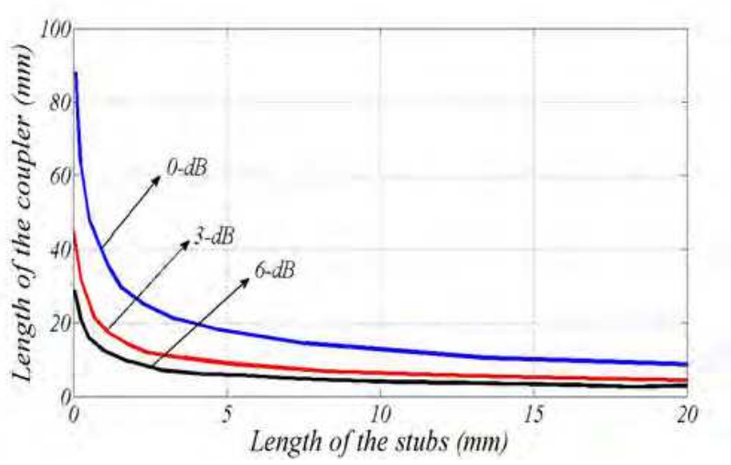

Fig. 20. Data for designing dimension of the proposed coupler on FR-4 substrate ($\varepsilon_r = 4.6$, $h = 1.6\,mm$) (Keshavarz et al., 2010).

Therefore, the proposed CLC is more compact than the microstrip coupler with the coupled-line length around $0.75\lambda_g$ presented in (Fujii & Ohta, 2005). Also, the width (W_s) and period distance (d_s) of the stubs are considered as: $W_s = 0.2\,mm$, $d_s = 0.6\,mm$ and the space between the stubs and transmission lines is 0.2 mm (i.e. $S = 0.2\,mm$).

The measured and simulated S-parameters of the proposed coupler are shown in Fig. 22. This figure shows the measured amplitude balance of ±2 dB over a bandwidth of 66% (2-4 GHz). In this figure, full-wave simulation and equivalent circuit model results have also been presented for verification. A good agreement between measurement, full-wave simulation and equivalent circuit model results is obtained and thus the usefulness of the presented equivalent circuit model is validated. The element values of the equivalent circuit model (Fig. 18) for the layout are: $L = 1.8\,nH$, $L_a = 3.2\,nH$, $C_a = 0.1\,pF$, $C_e = 0.2\,pF$ and $C_o = 1.8\,pF$.

In comparison with the conventional forward CLCs, the electrical length of the proposed CLC is more compact than CLCs presented in (Chang et al., 2001; Deng et al., 2002; Lauro et al., 2009). For instance, the coupled-line electrical length of the coupler is shortened to 50% of the conventional CLC electrical length reported in (Deng et al., 2002). Moreover, the bandwidth of the proposed CLC is wider than forward CLCs presented in (Deng et al., 2002; Lauro et al., 2009; Chang et al., 2001; Sen-Kuei & Tzong-Lin, 2010). For example, compared with the forward couplers reported in (Deng et al., 2002) and (Lauro et al., 2009), the proposed structure is capable of producing 65% bandwidth enhancement for the amplitude and a 0-dB coupling level with a smaller coupled-line length. Moreover, the proposed structure exhibits broader bandwidth than couplers presented in (Chang et al., 2001; Huang & Chu, 2010; Ikalainen & Matthaei, 1987; Sen-Kuei & Tzong-Lin, 2010; Lauro et al., 2009).

Fig. 23 shows the even- and odd-mode characteristic impedances computed using full-wave simulation. This result indicates that the proposed structure is matched to $50\,\Omega$ port impedance over the operating bandwidth, such that the additional tapered structure at each port for impedance matching can be eliminated. Hence, the proposed forward coupler would be more compact in size. As it was mentioned, for the proposed forward CLC, the coupler area is approximately constant. It means that reduction of the structure length results width increasing, proportionally (Fig. 20).

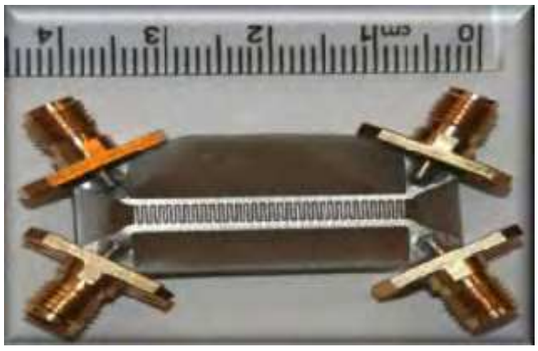

Fig. 21. Proposed forward symmetrical coupler which realized on FR-4 substrate ($\varepsilon_r = 4.6$, $h = 1.6\,mm$) (Keshavarz et al., 2010).

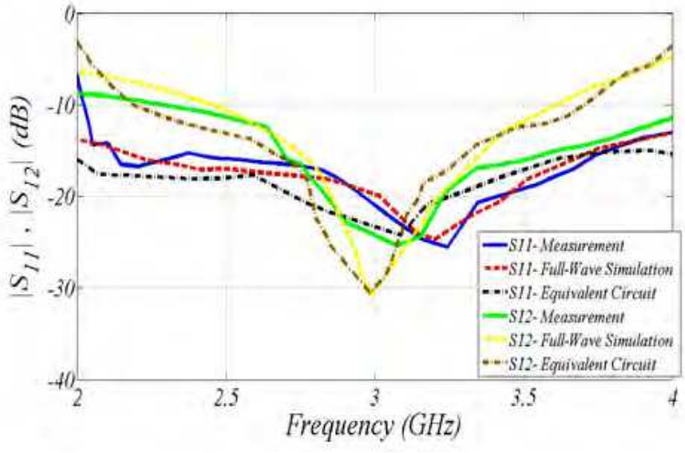

(a)

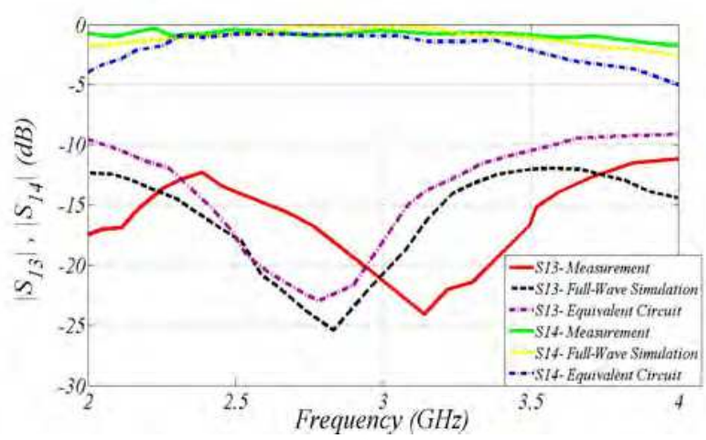

(b)

Fig. 22. Magnitude of the S-parameters, (a) S_{11}, S_{12} (b) S_{13}, S_{14} for the proposed coupler in Fig. 21 obtained by the full-wave simulation, equivalent circuit model and measurement results (Keshavarz et al., 2010).

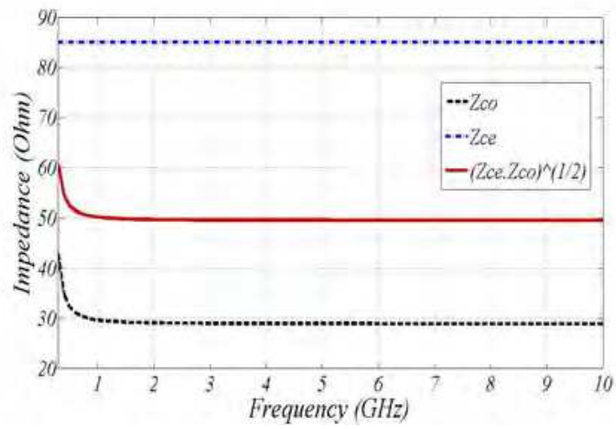

Fig. 23. Even and odd modes characteristic impedances of the coupler presented in Fig. 21 (Keshavarz et al., 2010).

4. Conclusion

In this chapter, some new techniques for realizing compact and tight coupling microstrip backward and forward CLCs with obtainable dimension, broad bandwidth and smaller size than the most conventional microstrip and CRLH couplers have been introduced. We presented three CLCs based on the concept of CRLH CLCs; a symmetrical backward CLC, an asymmetrical backward CLC and a symmetrical forward CLC.

New symmetrical backward coupler structure consists of only one interdigital capacitor in each coupled TL without shorted stubs as the CRLH TL. Designed and fabricated 3-dB microstrip coupler at center frequency about f_c = 3.2 GHz exhibits a matching (10-dB) bandwidth of over 2 GHz, a phase-balance (±10°) bandwidth of 1.3 GHz and at least 20-dB isolation between adjacent ports. The coupled-line length and the width of the proposed

structure are approximately, $\lambda_g/4$ and $\lambda_g/36$, respectively. Also, this coupler exhibits higher design simplicity than the existing CRLH CLCs.

Moreover, a new type of backward CLC composed of two different coupled lines, i.e. interdigital and conventional microstrip TLs has been proposed, fabricated, and investigated theoretically and experimentally. In this structure, an interdigital capacitor with only one finger is used as interdigital TL. This interdigital TL is coupled with a conventional microstrip TL and achieves an asymmetrical backward CLC. The proposed backward-wave coupler with 0.2 mm spacing between two coupled lines exhibits the amplitude balance of ±2 dB from 2.2 GHz to 4.2 GHz and the phase balance of 90^o±10^o from 2.2 GHz to 3.5 GHz.

Finally, a forward CLC composed of two identical microstrip TLs and periodic shunt stubs between them has been proposed and investigated experimentally and theoretically. Using loaded stubs between two microstrip coupled-lines forms the proposed 0-dB forward CLC which exhibits the amplitude balance of ±2 dB around center frequency of 3 GHz from 2 GHz to 4 GHz (66% bandwidth). A matching ($|S_{11}|$<15-dB) bandwidth of over 4 GHz (1-5 GHz) bandwidth and at least 15 dB isolation between adjacent ports have been seen in measurement results. In this forward-wave CLC, by increasing the length of the stubs, the coupler length decreases, proportionally.

5. References

Abdelaziz, A. F., Abuelfadl, T. M., & Elsayed, O. L. (2009). Realization of composite right/left-handed transmission line using coupled lines. *Progress In Electromagnetics Research*, Vol. 92, pp. 299–315.

Bahl, I. (2003). *Lumped Elements for RF and Microwave Circuits*, ArtechHouse, Boston.

Caloz, C. & Itoh, T. (2002). Application of the transmission line theory of left-handed (LH) materials to the realization of a microstrip LH transmission line. I*n Proc. IEEE-AP-S USNC/URSI National Radio Science Meeting,* vol. 2, pp. 412–415.

Caloz, C. & Itoh, T. (2004). A novel mixed conventional microstrip and composite right/left handed backward-wave directional coupler with broadband and tight coupling characteristics. *IEEE Microwave Wireless Component Letter,* vol. 14, no. 1, pp. 31-33.

Caloz, C. & Itoh, T. (2004). Transmission line approach of left-handed (LH) structuresand microstrip realization of a low-loss broadband LH filter. *IEEE Trans. Antennas Propagation*, vol. 52, no. 5, pp. 1159–1166.

Caloz, C., & Itoh, T. (2005). *Electromagnetic Metamaterials: Transmission Line Theory and Microwave Applications*, Wiley, New York.

Caloz, C., Sanada, A., & Itoh, T. (2004). A novel composite right/lefthanded coupled-line directional coupler with arbitrary coupling level and broad bandwidth. *IEEE Trans. Microwave Theory Technique*, vol. 52, pp. 980–992.

Chang, C., Qian, Y. & Itoh, T. (2001). Enhanced Forward Coupling Phenomena Between Microstrip Lines on Periodically Patterned Ground Plane. *IEEE MTT-S International Microwave Symposium Digest*, pp. 2039–2042.

Cristal, E.G. (1966). Coupled-Transmission-Line Directional Couplers with Coupled Lines of Unequal Characteristic Impedances. *G-MTT International Symposium Digest,* vol. 66 , no. 1, pp. 114 – 119.

Deng, J.D.S., Feng-ka H., Kuo, J.I., Kuo Y. H., Ching-Yuan L., & Chung-Sen W. (2002). Tightly coupling LTCC microwave coupled lines: analysis, modeling and realization Electronic Materials and Packaging. *Proceedings of the 4th International Symposium on Digital Object*, pp. 391 – 396.

Fouda, A.E., Safwat, A.M.E., & El-Hennawy, H. (2010). On the Applications of the Coupled-Line Composite Right/Left-Handed Unit Cell. *IEEE Transactions on Microwave Theory and Techniques*, vol. 58, no. 6, pp. 1584 – 1591.

Fujii, T. & Ohta, I. (2005). Size-Reduction of Coupled-Microstrip 3-dB Forward Couplers by Loading with Periodic Shunt Capacitive Stubs. *IEEE MTT-S International Microwave Symposium Digest,* pp. 1235–1238.

Garcia-Perez, O., Garcia Munoz, L. E., Segovia-Vargas, D., & Gonzalez-Posadas, V. (2010). Multiple order dual-band active ring filters with composite right/left-handed cells. *Progress In Electromagnetics Research*, vol. 104, 201–219.

Hirota, A., Tahara, Y., & Yoneda, N. (2009). A compact coupled-line forward coupler using composite right-/left-handed transmission lines. *IEEE MTT-S International Microwave Symposium Digest,* pp. 617 - 620.

Hirota, A., Tahara, Y., & Yoneda, N. (2011). A wide band forward coupler with balanced composite right-/left-handed transmission lines. *IEEE MTT-S International Microwave Symposium Digest,* pp. 1 – 4.

Huang, J.Q., & Chu, Q.X. (2010). Compact UWB band-pass filter utilizing modified composite right/left-handed structure with cross coupling. *Progress In Electromagnetics Research*, vol. 107, pp. 179–186.

Ikalainen, K., & Matthaei, L. (1987). Wide-Band, Forward-Coupling Microstrip Hybrids with High Directivity. *IEEE Trans. on Microwave Theory and Techniques*, vol. 35, no. 8, pp. 719–725.

Islam, R. & Eleftheriades, G. V. (2006). Printed high-directivity metamaterial MS/NRI coupled-line coupler for signal monitoring applications. *IEEE Microwave and Wireless Component Letter*, vol. 16, no. 4, pp. 164-166.

Islam, R., Elek, F., & Eleftheriades, G. V. (2004). Coupled line metamaterial coupler having co-directional phase but contradirectional power flow. *Electronics Letters*, vol. 40, no. 5, pp. 315–317.

Joon-Bum K., Chul-Soo K., Kwan-Sun C., Jun-Seok P., & Dal A. (2001). A design mapping formula of asymmetrical multi-element coupled line directional couplers. *IEEE MTT-S International Microwave Symposium Digest*, vol. 2, pp. 1293 - 1296.

Kawakami, T., Inoue, N., Horii, Y., & Kitamura, T. (2010). A super-compact 0dB/3dB forward coupler composed of multi-layered CRLH transmission lines with double left-handed shunt-inductors. *European Microwave Conference*, pp. 1409 – 1412.

Keshavarz, R., Movahhedi, M., Hakimi, A., & Abdipour, A. (2010). A Compact 0-dB Coupled-Line Forward Coupler by Loading with Shunt Periodic Stubs. *Asia Pacific Microwave Conference*, pp. 1248-1251.

Keshavarz, R., Movahhedi, M., Hakimi, A., & Abdipour, A. (2011). A novel broad bandwidth and compact backward coupler with high coupling-level. *Journal of Electromagnetic Waves and Applications,* vol. 25, no. 2/3, pp. 283-293.

Keshavarz, R., Movahhedi, M., Hakimi, A., & Abdipour, A. (2011). A broadband and compact asymmetrical backward coupled-line coupler with high coupling level. *Submitted to International Journal of Electronics and Communication.*

Lauro, S., Toscano, E. & Vegni, L. (2009). Symmetrical Coupled Microstrip Lines With Epsilon Negative Metamaterial Loading, *IEEE Transactions on Magnetics*, vol. 45, no. 7, pp. 1182-1189.

Mao, S. G. & Wu, M. S. (2007). A novel 3-dB directional coupler with Bandwidth and coupler with coupling-level, broad bandwidth and compact size using composite right/lefthanded coplanar waveguides. *IEEE Microwave Wireless Components Letter*, vol. 17, no. 5, pp. 331–333.

Mocanu, I.A., Militaru, N., Lojewski, G., Petrescu, T., & Banciu, M.G. (2010). Backward couplers using coupled composite right/left-handed transmission lines. *8th International Conference on Communications*, pp. 267 – 270.

Mongia, R., Bahl, I., & Bhartia, P. (1999). *RF and Microwave Coupledline Circuits*, Artech House, Norwood, MA.

Nguyen, H. V., & Caloz, C. (2006). Simple-design and compact MIM CRLH microstrip 3-dB coupled-line coupler. *Proc. IEEE International Microwave Symposium Digest*, pp. 1733–1736.

Pozar, M. D. (2004). *Microwave Engineering*, John Wiley & Sons.

Sen-Kuei, H. & Tzong-Lin W. (2010). A novel microstrip forward directional coupler based on an artificial substrate. *European Microwave Conference,* pp. 926-930.

Veselago, V. (1968). The electrodynamics of substances with simultaneously negative valuesof ε and μ. *Soviet Physics Uspekhi,* vol. 10, no. 4, pp. 509–514.

Wang, Y., Zhang, Y., Liu, F., He, L., Li, H., Chen, H., & Caloz, C. (2007). Simplified Description of Asymmetric Right-Handed Composite Right/Left-Handed Coupler in Microstrip-Chip Technology. *Microwave and Optical Technology Letters*, vol. 49, no. 9, pp. 2063-2068.

Zhang, Q., Khan, S. N., & Sailing, H. (2008) Coupled-line directional coupler based on Composite Right / Left-Handed coplanar waveguides. *International Workshop on Metamaterials*, pp. 301 – 304.

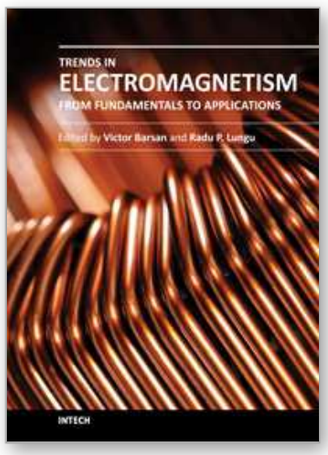

Trends in Electromagnetism - From Fundamentals to Applications
Edited by Dr. Victor Barsan

ISBN 978-953-51-0267-0
Hard cover, 290 pages
Publisher InTech
Published online 23, March, 2012
Published in print edition March, 2012

Among the branches of classical physics, electromagnetism is the domain which experiences the most spectacular development, both in its fundamental and practical aspects. The quantum corrections which generate non-linear terms of the standard Maxwell equations, their specific form in curved spaces, whose predictions can be confronted with the cosmic polarization rotation, or the topological model of electromagnetism, constructed with electromagnetic knots, are significant examples of recent theoretical developments. The similarities of the Sturm-Liouville problems in electromagnetism and quantum mechanics make possible deep analogies between the wave propagation in waveguides, ballistic electron movement in mesoscopic conductors and light propagation on optical fibers, facilitating a better understanding of these topics and fostering the transfer of techniques and results from one domain to another. Industrial applications, like magnetic refrigeration at room temperature or use of metamaterials for antenna couplers and covers, are of utmost practical interest. So, this book offers an interesting and useful reading for a broad category of specialists.

How to reference
In order to correctly reference this scholarly work, feel free to copy and paste the following:

Masoud Movahhedi and Rasool Keshavarz (2012). Coupled-Line Couplers Based on the Composite Right/Left-Handed (CRLH) Transmission Lines, Trends in Electromagnetism - From Fundamentals to Applications, Dr. Victor Barsan (Ed.), ISBN: 978-953-51-0267-0, InTech, Available from: http://www.intechopen.com/books/trends-in-electromagnetism-from-fundamentals-to-applications/coupled-line-couplers-based-on-the-composite-right-left-handed-crlh-transmission-lines

INTECH
open science | open minds

InTech Europe
University Campus STeP Ri
Slavka Krautzeka 83/A
51000 Rijeka, Croatia
Phone: +385 (51) 770 447
Fax: +385 (51) 686 166
www.intechopen.com

InTech China
Unit 405, Office Block, Hotel Equatorial Shanghai
No.65, Yan An Road (West), Shanghai, 200040, China
中国上海市延安西路65号上海国际贵都大饭店办公楼405单元
Phone: +86-21-62489820
Fax: +86-21-62489821

IntechOpen